International Journal of Chemistry and Materials Research
2015 Vol. 3, No. 10, 144-153.
ISSN(e): 2311-763X
ISSN(p): 2312-0991
DOI: 10.18488/journal.64/2015.3.10/64.10.144.153

REFORMING OF ETHANOL TO PRODUCE HYDROGEN OVER PTRU/CEO2 CATALYST

Josh Y.Z. Chiou[1] --- Jia-Lin Bi[2] --- Hsuan-Ying Kung[3] --- Chen-Bin Wang[4†]
[1,2,3,4]Department of Chemical and Materials Engineering, Chung Cheng Institute of Technology, National Defense University, Tahsi, Taiwan, ROC

ABSTRACT

The aim of this study is focused on the design of ethanol reforming catalyst to produce hydrogen at low-temperature with high ethanol conversion (X_{EtOH}), hydrogen yield (Y_{H_2}) and low CO distribution. A highly dispersed PtRu/CeO_2 catalyst is prepared by impregnation method. Catalytic performance and products distribution toward ethanol reforming reactions is evaluated in a fixed bed reactor. Three processes of ethanol reforming are performed: steam reforming of ethanol (SRE), partial oxidation of ethanol (POE) and oxidative steam reforming of ethanol (OSRE). The results show that the SRE reaction requires high temperature (T > 500 ℃) to achieve complete ethanol conversion, however, low temperature for both POE and OSRE (T < 300 ℃) reactions. Analytical results indicate the optimized molar ratios of O_2/EtOH and H_2O/EtOH are 0.44 and 4.9, respectively. Under this condition, the OSRE reaction over PtRu/CeO_2 catalyst is completely converted around 340 ℃ to get 2.3% CO and 4.1 mol H_2/mol EtOH.

Keywords: Reforming of ethanol, Partial oxidation of ethanol, Steam reforming of ethanol, Oxidative steam reforming of ethanol, Ceria-supported catalyst, Hydrogen.

Contribution/ Originality

The paper's primary contribution is finding that a highly active catalyst, PtRu/CeO_2, used in the reforming of ethanol is designed and evaluates for POE, SRE and OSRE reactions.

1. INTRODUCTION

Hydrogen produced from the oxygenated hydrocarbons has most used in recent years. Alcohol is better candidate among several oxygenated fuels. Methanol has been attracted great interest for potential application in fuel cells [1] however, there are health issue and environmental impacts on the utilization of methanol. Compared with methanol, ethanol possesses many distinguishing features such as lower toxicity, higher hydrogen content, more

† Corresponding author

environmental protection and as renewable-energy from several biomass sources [2, 3]. Hydrogen production can be obtained from various reforming processes, i.e. ethanol decomposition (DE), steam reforming of ethanol (SRE), partial oxidation of ethanol (POE) and oxidation steam reforming of ethanol (OSRE) reactions.

Low temperature SRE over supported noble catalysts was investigated by Basagiannis, et al. [4]. The catalytic performance varied in the order of Pt > Pd > Rh > Ru which had been found, where Pt was an excellent catalyst toward hydrogen production with high activity and selectivity. Not only for the SRE, but also active on the POE [5] OSRE [6] and water-gas-shift (WSG) [7] reactions. However, the price of Pt is much more cost; Ru is considered as a less costly active catalyst. Supported noble metal catalyst, i.e. Ru/Al_2O_3 had been used on hydrogen production from ethanol by reforming reaction with low metal loading [3, 4]. Byrd et al. carried out the reforming of ethanol [8] and glycerol [9] in supercritical water over Ru/Al_2O_3 to produce hydrogen at high pressure with a short reaction time less than 5 s. The hydrogen yield increases with temperature (above 700 °C) and pressure has a negligible effect in the supercritical region.

Ceria-supported noble metal catalysts had been widely used upon the reforming reaction and possessed catalytic performance [10, 11]. This is attributed to the preferential reducibility and oxygen storage-release capacity that the deposited coke can be gasification easily preventing the deactivation of catalysts under steam condition. Noble metal catalysts with ceria support can promote the WGS reaction leading to lower the production of CO and increase the yield of H_2 [12, 13]. Moreover, ceria also improves the dispersion of the active phases [14] or the formation of oxide solid solution [15]. Both Pt/CeO_2 and Ru/CeO_2 catalysts had been shown to possess significant activity for the SRE reaction. Recently, Ciambelli, et al. [16] studied a highly active and selective Pt/CeO_2 catalyst for low temperatures SRE with negligible CO production. Moreover, Pt/Al_2O_3 also was chosen as a reference catalyst to investigate the deposited coke by the temperature programmed oxidation (TPO) technique, and found that more stable carbonaceous species deposited on Pt/Al_2O_3 catalyst. De Lima, et al. [17] reported that two approached methods can improve the stability of Pt/CeO_2 catalyst for SRE reaction, i.e. addition of tin (Sn) to suppress deposited carbon and co-feeding of CO_2 to compete the adsorption sites between ethanol and CO_2 for in promoting catalytic stability.

In our previous research, zirconia-supported platinum group catalysts (Pt, Ru and PtRu) for low temperature OSRE were evaluated [18]. The bimetallic $PtRu/ZrO_2$ catalyst exhibited better catalytic performance than the single metal catalysts (Pt/ZrO_2 and Ru/ZrO_2). Furthermore, the addition of sodium as a promoter to modify the $PtRu/ZrO_2$ catalyst showed the best active on OSRE at temperature as low as 300 °C and produced less CO (< 0.2%) at temperature lower than 340 °C [19]. Furthermore, the support also strongly affected the catalytic performance of supported metal catalysts in reforming reaction to produce hydrogen [20]. In this paper, the study of hydrogen production from SRE, POE and OSRE reforming processes over the $PtRu/CeO_2$ catalyst is studied.

2. EXPERIMENTAL

2.1. Catalyst Preparation

A precipitation method was used for the preparation of CeO_2 support using $Ce(NO_3)_3 \cdot 6H_2O$ (Showa) as precursor. It was thoroughly dissolved in water and the solution was precipitated with the addition of Na_2CO_3 (to maintain the pH of 9). After drying at 110 °C and calcination at 400 °C, the prepared CeO_2 powder was stored as support (surface area is 106 $m^2 \cdot g^{-1}$). Ceria-supported PtRu catalyst was prepared with impregnating the support by using H_2PtCl_6 and $RuCl_3$ as precursors. The loading of $PtRu/ZrO_2$ catalyst was 1.5 wt% for each component. After drying at 110 °C and calcination under 400 °C for 4 h, prepared sample was crushed to 60 ~ 80 mesh and stored as fresh catalyst (surface area is 104 $m^2 \cdot g^{-1}$).

2.2. Catalyst Characterization

Both Pt (1.38 wt%) and Ru (1.34 wt%) loading in the fresh catalyst were determined by the atomic-emission technique using an ICP-MS (Perkin–Elmer). BET surface area (S_{BET}) measurement was conducted using a Micromeritics ASAP 2010 instrument. The catalyst was pre-outgassed in a vacuum for 3 h at 110 °C. The surface area was determined from the nitrogen adsorption isotherm. X-ray diffraction (XRD) measurement was performed using a MAC Science MXP18 diffractometer with Cu $K_{\alpha 1}$ radiation (λ = 1.5405 Å) at 40 kV and 30 mA. The microstructure and particle size of the reduced catalysts was observed, using transmission electron microscopy (TEM) with a JEM-2010 microscope (JEOL), at an acceleration voltage of 200 kV. During the TPR experimental, about 50 mg sample was heated in a flow of 10% H_2/N_2 gas mixture at a flow rate of 10 $ml \cdot min^{-1}$. The temperature was programmed to rise with 7 $°C \cdot min^{-1}$ from −80 to 190 °C. The amount of the consumed H_2 was monitored continuously with a thermal conductivity detector (TCD).

2.3. Catalytic Activity Measurement

Catalytic activities of prepared sample towards POE, SRE and OSRE reactions were tested in a fixed-bed flow reactor at atmospheric pressure. For each run, approximately 100 mg catalyst was packed in a 4 mm i.d. quartz tubular reactor and held by glass-wool plugs. Before reaction, the catalyst was activated by reduction in hydrogen at 200 °C for 3 h. Temperature of the reactor was controlled by a heating tape and measured by a thermocouple (1.2 mm i.d.) at the center of the reactor bed. The catalytic activity of $PtRu/CeO_2$ catalyst towards ethanol reforming was under the molar ratio of $O_2/EtOH$ = 0.5 for POE, $H_2O/EtOH$ = 13 for SRE, $O_2/EtOH$ = 0.44 and $H_2O/EtOH$ = 4.9 for OSRE, respectively, which carried out at atmospheric pressure and 290 ~ 520 °C. The outlet gas was analyzed by the gas chromatography (GC) with MS-5A (for detecting H_2, CH_4 and CO) and Porapak Q columns (for detecting CO_2, H_2O, C_2H_4, CH_3CHO, CH_3COCH_3 and C_2H_5OH).

3. RESULTS AND DISCUSSION

3.1. Catalyst Characterization

X-ray diffraction is employed to identify the crystalline phases in the catalyst. Figure 1 shows the XRD patterns of CeO_2 support and $PtRu/CeO_2$ catalyst to identify the crystalline phases. The patterns show a well-crystallized CeO_2 phase with a fluorite-type structure. The XRD profile of $PtRu/CeO_2$ displays a similar diffraction pattern to that of CeO_2 support, and no significant diffraction signal of Pt (111) or PtRu (111) is observed, perhaps the corresponding particles well-dispersed on the surface of ceria are below the detection limit of XRD. Figure 2 displays TEM image of the particle size distribution of $PtRu/CeO_2$catalyst. Pt and Ru, and/or PtRu-alloy particles are found uniformly dispersed on the surface of ceria support, which also is convinced with XRD analysis. The attached histograms are size distribution and determined by directly measuring the size of 100 particles from many parts of the magnified TEM photographs. The calculated mean diameter of particles is 3.3 nm.

Figure 3 shows the TPR profiles of CeO_2 support and Pt/CeO_2, Ru/CeO_2 and $PtRu/CeO_2$ catalysts. Pure CeO_2 support presents reduction peaks (T_r) around 420 and 735 °C. The first peak is attributed to the removal of surface capping oxygen during the reduction reaction and the second peak is related to the reduction of bulk CeO_2 [21, 22]. The Pt/CeO_2, Ru/CeO_2 and $PtRu/CeO_2$ catalysts exhibit the reduction signal at 65, 130 and 16 °C, respectively. A comparison of these TPR traces reveals that the T_r of $PtRu/CeO_2$ is lower than those of Pt/CeO_2 and Ru/CeO_2, perhaps because the formation oxide of PtRu alloy, which shifts the reduction to lower temperature.

3.2. Catalytic Performance of Ethanol Reforming

3.2.1. Partial Oxidation of Ethanol

The partial oxidation of ethanol has been investigated at 300 – 410 °C. Within the temperature ranges, oxygen was completely consumed. Except the minor C_2H_4 (< 0.5%) and CH_4 (< 3.5%), the predominant components in the reaction product are H_2, H_2O, CO and CO_2. Figure 4 presents the catalytic performance in the POE reaction under O_2/EtOH ratio of 0.5 over $PtRu/CeO_2$ catalyst. The ethanol conversion (X_{EtOH}) is complete within the test temperatures (T_R). However, both H_2 and CO_2 distribution are drastically dropped with increasing T_R, while increases for the distribution of CO. The variation may be attributed to an increase of the rate of reaction with T_R. Initially, the dehydrogenation and decomposition of acetaldehyde occurs rapidly. The adsorbed CO (CO_{ad}) may be desorbed (for the weakly adsorbed) or oxidized by the lattice oxygen (O_L) or adsorbed oxygen on the active metal.

$$C_2H_5OH \rightarrow CH_3CHO + H_2 \quad (1)$$

$$CH_3CHO \rightarrow CO_{ad} + CH_4 \quad (2)$$

$$CO_{ad} \rightarrow CO \quad (3)$$

$$CO_{ad} + O_L \rightarrow CO_2 \quad (4)$$

The dropping of H_2 may be attributed to the competitive oxidation of H_2 with CO which is priority than the oxidation of CO as the following reaction.

$$H_2 + 1/2\ O_2 \rightarrow H_2O \qquad (5)$$

Breen, et al. [23] reported that zirconia-supported Pt catalysts were much more active than the corresponding alumina-supported Pt catalysts in the production of hydrogen by steam reforming of ethanol. This indicates that the oxygen storage and releasing capacity on reducible oxide like ZrO_2 can promote the migration of lattice oxygen to the Pt surface to selective oxidation of CO [24, 25]. On the other hand, the adsorbed oxygen on the Pt surface of a non-reducible oxide like Al_2O_3 is less active for the selective oxidation of CO. Although CeO_2 is a reducible oxide, the CO distribution increases with the T_R.

3.2.2. Steam Reforming of Ethanol

The catalytic performance of $PtRu/CeO_2$ catalyst in the steam reforming of ethanol under 300 – 520 °C is described in Figure 5. From the distribution of very minor C_2H_4 (< 0.1% at lower temperature) with T_R, we exclude the side-reaction of ethanol dehydration to ethylene. Ethanol conversion and H_2 production increase progressively with T_R. The X_{EtOH} is complete as the T_R approaching 400 °C. Under high conversion distribution, high selectivity to H_2 is achieved. At lower temperature (< 400 °C), the reaction follows an ethanol dehydrogenation to acetaldehyde and hydrogen, and then advances the decomposition of acetaldehyde into methane and CO. At middle temperature (400 < T_R < 500 °C), the decrease of CH_4 and increase of H_2 are observed. Since there is no carbon deposition associated with the used catalyst, it indicates the steam reforming of methane (SRM) and water gas shift (WGS) reaction occurs simultaneously.

$$CH_4 + H_2O \rightarrow CO + 3\ H_2 \qquad (6)$$

$$CO + H_2O \rightarrow CO_2 + H_2 \qquad (7)$$

At higher temperature (> 500 °C), the decrease of H_2 and CO_2 going with the increase of CO demonstrates that the reversed water gas shift (RWGS) reaction occurs.

$$CO_2 + H_2 \rightarrow CO + H_2O \qquad (8)$$

Comparison the T_R and yield of hydrogen (Y_{H2}) among different reforming processes, the POE reaction initiates at low temperature and is an auto-thermal procedure, while high temperature stimulates for the SRE reaction. The disadvantage of POE reaction attributes to the high distribution of CO and low Y_{H2} since the accompanied side-reaction of oxidation of hydrogen occurs simultaneously. The maximum Y_{H2} (approaches 2.5) obtains at 300 °C for the POE reaction. The advantage of SRE reaction attributes to the low distribution of CO and high Y_{H2} since the accompanied side-reactions of SRM and WGS occurs simultaneously. The maximum Y_{H2} (approaches 5.0) obtains at 500 °C for the SRE reaction.

3.2.3. Oxidative Steam Reforming of Ethanol

Figure 6 displays the X_{EtOH}, products distribution (water excluded) and Y_{H2} from OSRE with a EtOH/H_2O/O_2 at a molar ratio of 1:4.9:0.44 over a PtRu/CeO_2 catalyst between 290 and 380 °C. Ethanol is completely converted over the entire temperature range. The distribution of H_2 and CO_2 products increase with temperature, whereas CH_4 and CO are minor (< 3%). This demonstrates that the decomposition of acetaldehyde is active at low temperature for the OSRE reaction which derives only C_1 species and H_2. At lower temperature (< 340 °C), the main reaction follows the dehydrogenation and decomposition of acetaldehyde into methane and CO. Also, the side-reaction of WGS occurs associated. At higher temperature (> 340 °C), the decrease of H_2 and increase of CO_2 demonstrates that the combustion of hydrogen and oxidation of CO occurs simultaneously. Figure 7 summarizes the Y_{H2} and S_{CO} over PtRu/CeO_2 catalyst for the reforming of ethanol under various temperatures. The results show that the SRE reaction requires higher temperature (T_R ~ 400 °C) to achieve complete ethanol conversion than both POE and OSRE reactions (T_R ~ 300 °C). The distribution of CO is minor for both SRE and OSRE reactions (< 2.5% for SRE, < 3% for OSRE). This demonstrates that the WGS is an important side-reaction in the reforming of ethanol to produce H_2 and CO_2. A comparison of the temperature of WGS (T_{WGS}) shows that it is lower for both SRE and OSRE reaction (T_{WGS} < 350 °C). The Y_{H2} is lower for the POE reaction than both SRE and OSRE reactions. At low temperature, the Y_{H2} approaches 4.1 for the OSRE reaction at T_R around 340 °C. On the other hand, the Y_{H2} approaches 5.0 for the SRE reaction at T_R around 500 °C. This investigation clearly indicates that the OSRE reaction is more efficient at a lower operating temperature (T_R < 350 °C).

4. CONCLUSIONS

A highly active catalyst, PtRu/CeO_2, used in the reforming of ethanol was designed and evaluated for POE, SRE and OSRE reactions. The results demonstrated that the distribution of CO was minor for both SRE and OSRE reactions (< 2.5% for SRE, < 3% for OSRE). The higher temperature (T_R ~ 400 °C) was required for the SRE reaction to achieve complete conversion than the OSRE reaction (T_R ~ 300 °C). Also, the lower Y_{H2} was produced for the POE reaction (Y_{H2} approaches 2.5) than both SRE and OSRE reactions (Y_{H2} approaches 5 and 4.1).

5. ACKNOWLEDGEMENT

We are pleased to acknowledge the financial support for this study from the Ministry of Science and Technology of the Republic of China under contract numbers of MOST 104-2119-M-606-001-..

REFERENCES

[1] S. Wasmusa and A. Küver, "Methanol oxidation and direct methanol fuel cells: A selective review," *J. Electroanal. Chem.*, vol. 461, pp. 14-31, 1999.

[2] R. D. Cortright, R. R. Davda, and J. A. Dumesic, "Hydrogen from catalytic reforming of biomass-derived hydrocarbons in liquid water," *Nature*, vol. 418, pp. 964-967, 2002.

[3] D. K. Liguras, D. I. Kondarides, and X. E. Verykios, "Production of hydrogen for fuel cells by steam reforming of ethanol over supported noble metal catalysts," *Appl. Catal. B.*, vol. 43, pp. 345-354, 2003.

[4] A. C. Basagiannis, P. Panagiotopoulou, and X. E. Verykios, "Low temperature steam reforming of ethanol over supported noble metal catalysts," *Top. Catal.*, vol. 51, pp. 2-12, 2008.

[5] J. R. Salge, G. A. Deluga, and L. D. Schmidt, "Catalytic partial oxidation of ethanol over noble metal catalysts," *J. Catal.*, vol. 235, pp. 69-78, 2005.

[6] A. Gutierrez, R. Karinen, S. Airaksinen, R. Kaila, and A. O. L. Krause, "Autothermal reforming of ethanol on noble metal catalysts," *Int. J. Hydrogen Energy*, vol. 36, pp. 8967-8977, 2011.

[7] C. M. Kalamaras, I. D. Gonzalez, R. M. Navarro, J. L. G. Fierro, and A. M. Efstathiou, "Effects of reaction temperature and support composition on the mechanism of water-gas shift reaction over supported-Pt catalysts," *J. Phy. Chem. C.*, vol. 115, pp. 11595-11610, 2011.

[8] A. J. Byrd, K. K. Pant, and R. B. Gupta, "Hydrogen production from ethanol by reforming in supercritical water using Ru/Al_2O_3 catalyst," *Energy and Fuels*, vol. 21, pp. 3541-3547, 2007.

[9] A. J. Byrd, K. K. Pant, and R. B. Gupta, "Hydrogen production from glycerol by reforming in supercritical water over Ru/Al_2O_3 catalyst," *Fuel*, vol. 87, pp. 2956-2960, 2008.

[10] E. P. Murray, T. Tsai, and S. A. Barnett, "A direct-methane fuel cell with a ceria-based anode," *Nature*, vol. 400, pp. 649-651, 1999.

[11] G. A. Deluga, J. R. Salge, L. D. Schmidt, and X. E. Verykios, "Renewable hydrogen from ethanol by autothermal reforming," *Science*, vol. 303, pp. 993-997, 2004.

[12] C. Wheeler, A. Jhalani, E. J. Klein, S. Tummala, and L. D. Schmidt, "The water-gas-shift reaction at short contact times," *J. Catal.*, vol. 223, pp. 191-199, 2004.

[13] G. Jacobs, P. M. Patterson, U. M. Graham, D. E. Sparks, and B. H. Davis, "Low temperature water-gas shift: Kinetic isotope effect observed for decomposition of surface formates for Pt/ceria catalysts," *Appl. Catal. A.*, vol. 269, pp. 63-73, 2004.

[14] Y. Li, Q. Fu, and M. Flytzani-Stephanopoulos, "Low-temperature water-gas shift reaction over Cu- and Ni-loaded cerium oxide catalysts," *Appl. Catal. B.*, vol. 27, pp. 179-190, 2000.

[15] C. Lamonier, A. Ponchel, A. D. Huysser, and L. Jalowiecki-Duhamel, "Studies of the cerium-metal oxygen hydrogen system metal = Cu, Ni," *Catal. Today*, vol. 50, pp. 247-259, 1999.

[16] P. Ciambelli, V. Palma, and A. Ruggiero, "Low temperature catalytic steam reforming of ethanol. 1. The effect of the support on the activity and stability of Pt catalysts," *Appl. Catal. B.*, vol. 96, pp. 18-27, 2010.

[17] S. M. De Lima, A. M. Da Silva, G. Jacobs, B. H. Davis, L. V. Mattos, and F. B. Noronha, "New approaches to improving catalyst stability over Pt/ceria during ethanol steam reforming: Sn addition and CO_2 co-feeding," *Appl. Catal. B.*, vol. 96, pp. 387-398, 2010.

[18] J. L. Bi, Y. Y. Hong, C. C. Lee, C. T. Yeh, and C. B. Wang, "Novel zirconia-supported catalysts for low-temperature oxidative steam reforming of ethanol," *Catal. Today*, vol. 129, pp. 322-329, 2007.

[19] C. H. Wang, K. F. Ho, J. Y. Z. Chiou, C. L. Lee, S. Y. Yang, C. T. Yeh, and C. B. Wang, "Oxidative steam reforming of ethanol over PtRu/ZrO_2 catalysts modified with sodium and magnesium," *Catal. Commun.*, vol. 12, pp. 854-858, 2011.

[20] C. B. Wang, J. L. Bi, S. N. Hsu, and C. T. Yeh, "Low-temperature mild partial oxidation of ethanol over supported platinum catalysts," *Catal. Today*, vol. 129, pp. 330-335, 2007.

[21] G. R. Rao, H. R. Sahu, and B. G. Mishra, "Surface and catalytic properties of Cu-Ce-O composite oxides prepared by combustion method," *Colloids Surf. A.*, vol. 220, pp. 261-269, 2003.

[22] A. Trovarelli, "Catalytic properties of ceria and CeO_2-containing materials," *Catal. Rev. Sci. Eng.*, vol. 38, pp. 439-520, 1996.

[23] J. P. Breen, R. Burch, and H. M. Coleman, "Metal-catalysed steam reforming of ethanol in the production of hydrogen for fuel cell applications," *Appl. Catal. B.*, vol. 39, pp. 65-74, 2002.

[24] E. J. Walter, S. P. Lewis, and A. M. Rappe, "First principles study of carbon monoxide adsorption on zirconia-supported copper," *Surf. Sci.*, vol. 495, pp. 44-50, 2001.

[25] A. Manasilp and E. Gulari, "Selective CO oxidation over Pt/alumina catalysts for fuel cell applications," *Appl. Catal. B.*, vol. 37, pp. 17-25, 2002.

Figure captions

1. XRD patterns of CeO_2 and PtRu/CeO_2.
2. TEM images and histograms of the particle size distribution of PtRu/CeO_2 catalyst.
3. TPR profiles of: (a) CeO_2 (b) PtRu/CeO_2 (c) Pt/CeO_2 and (d) Ru/CeO_2.
4. Catalytic performance in the POE reaction over PtRu/CeO_2 catalyst.
5. Catalytic performance in the SRE reaction over PtRu/CeO_2 catalyst.
6. Catalytic performance in the OSRE reaction over PtRu/CeO_2 catalyst.
7. Y_{H2} and CO distribution for ethanol reforming reaction under various temperatures.

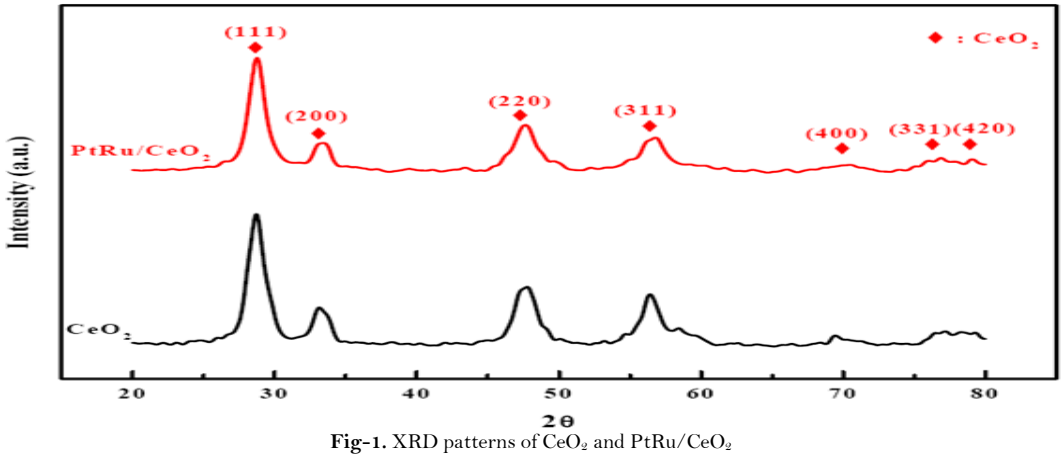

Fig-1. XRD patterns of CeO_2 and PtRu/CeO_2

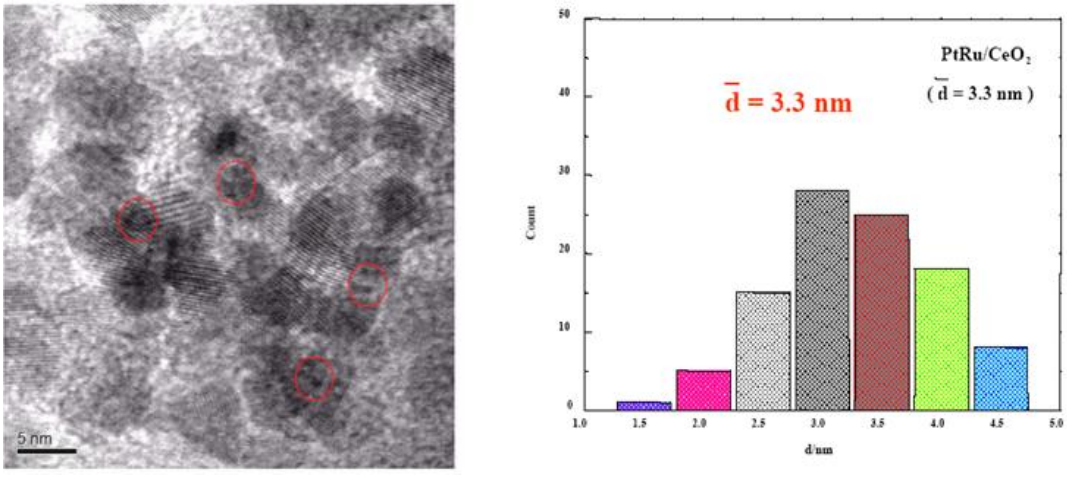

Fig-2. TEM images and histograms of the particle size distribution of $PtRu/CeO_2$ catalyst

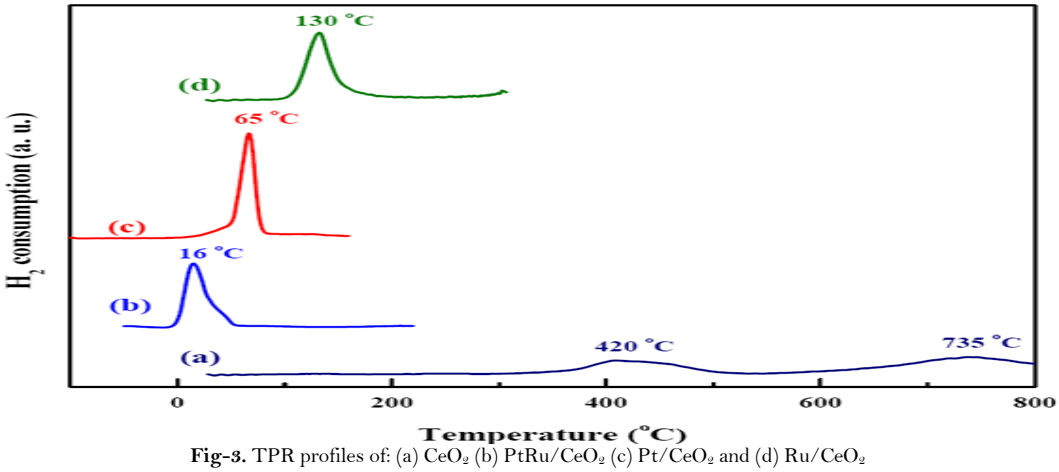

Fig-3. TPR profiles of: (a) CeO_2 (b) $PtRu/CeO_2$ (c) Pt/CeO_2 and (d) Ru/CeO_2

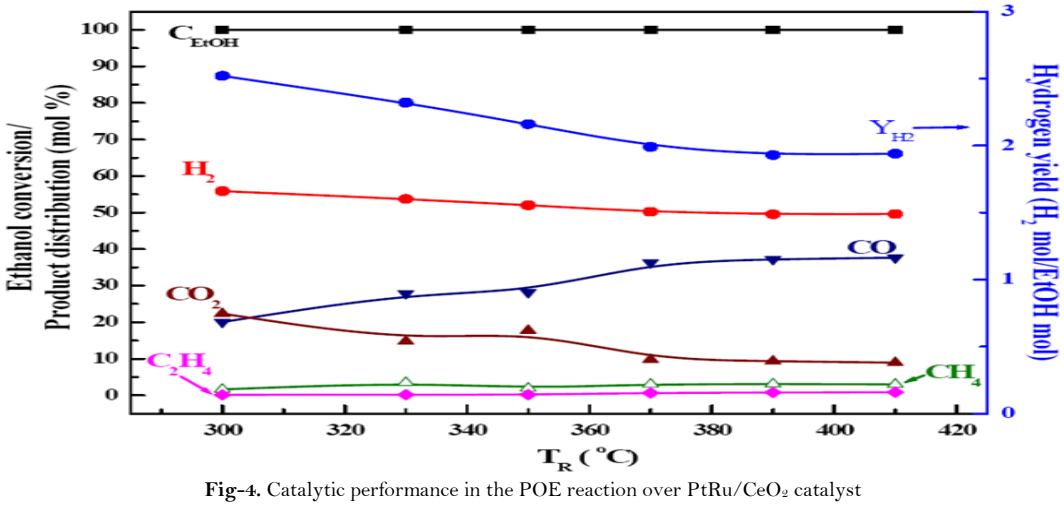

Fig-4. Catalytic performance in the POE reaction over $PtRu/CeO_2$ catalyst

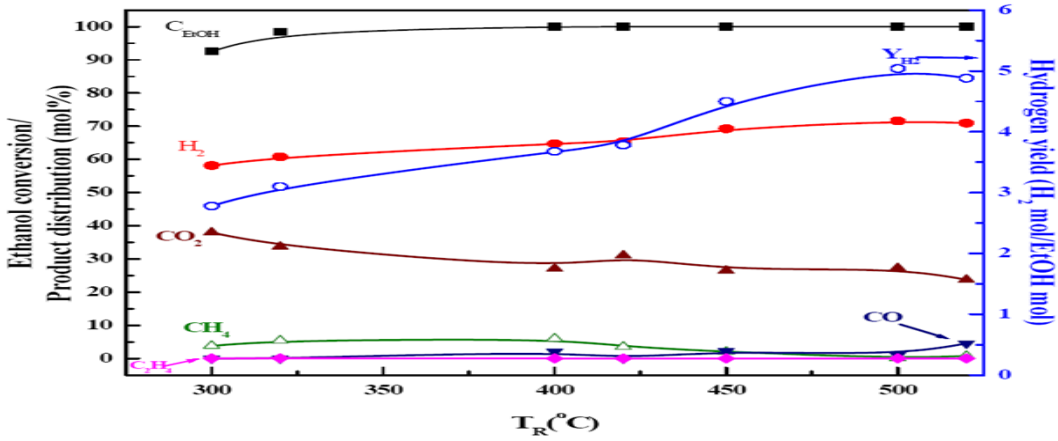

Fig-5. Catalytic performance in the SRE reaction over $PtRu/CeO_2$ catalyst

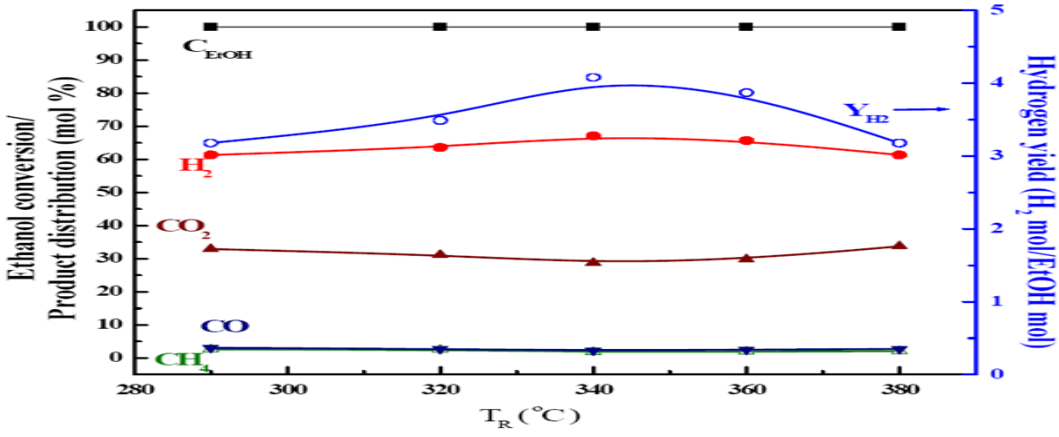

Fig-6. Catalytic performance in the OSRE reaction over $PtRu/CeO_2$ catalyst

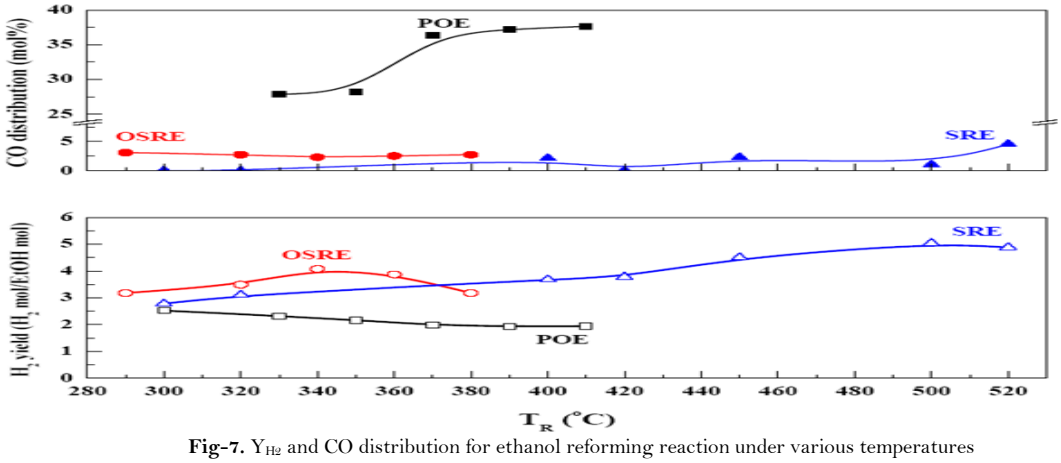

Fig-7. Y_{H2} and CO distribution for ethanol reforming reaction under various temperatures